

Camera Movement Estimation and Path Correction using the Combination of Modified A-SIFT and Stereo System for 3D Modelling

Usha Kumari¹ and Shuvendu Rana¹

¹SRM University AP, Computer Science & Engineering,
Mangalagiri, Neerukonda, Guntur, 522240, Andhra Pradesh,
India.

Contributing authors: usha_kumari@srmmap.edu.in;
shuvendu@ieee.org;

Abstract

Creating accurate and efficient 3D models poses significant challenges, particularly in addressing large viewpoint variations, computational complexity, and alignment discrepancies. Efficient camera path generation can help resolve these issues. In this context, a modified version of the Affine Scale-Invariant Feature Transform (ASIFT) is proposed to extract more matching points with reduced computational overhead, ensuring an adequate number of inliers for precise camera rotation angle estimation. Additionally, a novel two-camera-based rotation correction model is introduced to mitigate small rotational errors, further enhancing accuracy. Furthermore, a stereo camera-based translation estimation and correction model is implemented to determine camera movement in 3D space by altering the Structure From Motion (SFM) model. Finally, the novel combination of ASIFT and two camera-based SFM models provides an accurate camera movement trajectory in 3D space. Experimental results show that the proposed camera movement approach achieves 99.9% accuracy compared to the actual camera movement path and outperforms state-of-the-art camera path estimation methods. By leveraging this accurate camera path, the system facilitates the creation of precise 3D models, making it a robust solution for applications requiring high fidelity and efficiency in 3D reconstruction.

Keywords: Simultaneous Localization and Mapping, Structure From Motion, multi-view, Affine SIFT

1 Introduction

Technological transitions have been evolving over the past few years. One such revolution can be seen in the landscape of 3D modeling. The role of 3D modeling is crucial in various industries, as it visualizes a product or concept before it is physically made, saving both time and resources. In the context of this field, an accurate 3D modeling technique becomes even more important. Recently, cameras using Simultaneous Localization and Mapping (SLAM) [1] have been employed to create 3D structures. The main challenge in this process is creating and detecting the camera movement path. Due to the use of non-rigid cameras for 3D model creation, proper camera localization techniques have become an important research area. In this regard, Structure From Motion (SFM) [2] plays an important role in estimating the camera movement path. However, the primary issue is that estimating accurate world coordinate mapping using SFM becomes difficult due to the non-rigid movement of the camera. Moreover, the presence of incorrect inliers in the SFM model leads to errors in camera position estimation. In 3D modeling technique, many works have been carried out [1–30]. Some of the works are based on 3D surface estimation, Camera positioning and Non-rigid object localization [29].

In the realm of three-dimensional reconstruction, accurate surface estimation is crucial. This becomes even more important when dealing with objects that have complex surface characteristics, such as specular reflectance. In this area, Jiang Yu Zheng et al. [2] propose a 3D reconstruction method that utilizes object rotation and extended lighting. This method is based on linear equations for camera motion and surface estimation. However, the approach is sensitive to changes in lighting and faces challenges with shadows, rough surfaces, and complex geometries.

In order to determine the best camera placement, Robert Bodor et al. [26] present an optimization strategy that balances coverage and resolution by adjusting camera settings iteratively based on motion statistics. The method is effective but can be computationally expensive, particularly in complex multi-camera setups. Ware and Osborne [27] highlighted the difficulty of using six-degree-of-freedom (DOF) methods for 3D camera control with 2D inputs, which led Hachet et al. [28] to develop the Navidget approach for simplified control. Navidget is more effective and intuitive, especially with its circular metaphor for camera movement. However, it may struggle in crowded situations with frequent occlusions and requires more processing power. Using the pixel-wise eigenspace method, Arif and Vela [29] propose a method for non-rigid object localization and segmentation, enhancing deformation resilience through mean-shift iterations and similarity measures, despite facing challenges with significant appearance changes and severe occlusions. Similarly, Comanicu et al. [30] present a non-rigid object localization technique based on color models and the mean-shift algorithm, yet face difficulties in dynamic scenes with occlusion or dynamic environments. On the other hand, in the case of SLAM-based techniques, Lu and Milios [4] presented a graph-based

method for mapping using odometry and scan alignment, optimizing pose relations through scan matching. However, it relies heavily on accurate camera positioning systems. Furthermore, S. Thrun and M. Montemerlo [5] introduced Graph SLAM for offline SLAM by converting the SLAM posterior into a graphical network, using GPS data and variable elimination. However, it is limited by its assumption of independent Gaussian noise. Andrew J. Davison et al. [6] present a real-time algorithm for 3D trajectory recovery of a monocular camera, achieving drift-free SLAM performance. However, it lacks an in-depth discussion on real-world implementation challenges and sensor noise. Brian Williams et al. [7] developed a real-time monocular SLAM system using RANSAC and online learning. However, it struggles with relocalization beyond 80 features, complexity in large maps, and potential feature drift. Hauke Strasdat et al. [8] compare filtering and sparse bundle adjustment for visual SLAM using Monte Carlo experiments, emphasizing accuracy and cost. However, they overlook large-scale SLAM, loop closing, and the impact of the visual front end. Similarly, in this field, Raúl Mur-Artal et al. [9] introduce a real-time monocular SLAM system using ORB features for robust tracking and mapping. However, it can be complex for new users, resource-intensive, and has limited testing in extreme conditions. Erik Sandström [10] proposes a dense visual SLAM method with an adaptive point-based neural scene representation for improved accuracy and efficiency. However, it faces challenges related to complexity, resource demands, and generalizability. Fayad et al. [12] propose a quadratic deformation model for non-rigid SFM, enhancing 3D reconstruction of complex deformations. However, it requires precise initial estimates and careful parameter tuning. Paulo F. U. Gotardo and Aleix M. Martinez [13] presented a novel Non-Rigid Structure-from-Motion technique using complementary rank-3 spaces for improved shape reconstruction. However, it faces challenges with complex shapes, occlusions, resource demands, and generalizability. Suryansh Kumar et al. [14] present a method for multi-body non-rigid SFM, enabling simultaneous segmentation and reconstruction of non-rigid structures. However, it faces challenges related to computational complexity, parameter sensitivity, and limited generalization. Agniva Sengupta and Adrien Bartoli [15] introduce a tubular NRSfM method for improved 3D reconstruction in colonoscopy, achieving a 71.74% improvement. However, it faces challenges with weak textures and unstable geometry. M. J. Westoby et al. [16] highlight the cost-effectiveness of SFM photogrammetry for high-resolution topographic reconstruction in geoscience. However, they note limitations in error analysis, processing times, and performance in densely vegetated areas. Martínez-Espejo Zaragoza et al. [17] integrate SFM, TLS, and UAV photogrammetry for 3D modeling in remote areas for disaster response, highlighting challenges with non-perpendicular surfaces and vertical feature capture. Yuan et al. [18] enhance 3D modeling efficiency through video-based keyframe extraction. However, their approach relies on accurate keyframe selection and faces challenges with incomplete video data and the trade-off between detail and processing speed. Granshaw [31] traces the evolution of SFM, highlighting its

geoscience applications with consumer cameras but noting challenges in achieving the required image overlap. Nesbit and Hugenholtz [19] examine 3D model accuracy in high-relief landscapes using UAV-based oblique images in UAV-based SFM, comparing it to TLS. However, their approach faces limitations with Pix4D mapper, surface deformation, and optimal oblique imaging setups. Xiao et al. [20] propose an SFM method using coordinate MLPs to improve 3D reconstruction from 2D correspondence biases. Nevertheless, they encounter challenges with occlusions, dynamic scenes, and scalability due to computational demands. Chen et al. [21] present an end-to-end multi-view SfM model that enhances 3D reconstruction accuracy using hypercorrelation volumes and RAFT-based feature matching. However, its complexity may hinder real-time applications and its use on resource-limited devices. Tulsiani et al. [32] propose the Layered Depth Image (LDI) framework, which infers multi-layered 3D representations from single images, addressing stereo limitations. However, it struggles with complex geometries and occlusions, particularly when multi-view images for training are limited. Yan Wang et al. [33] propose PLUMENet, a stereo-based 3D detector that utilizes pseudo LiDAR feature volumes for improved depth estimation. However, its reliance on stereo images and high computational demands limit its applicability in resource-constrained environments. Haozhe Xie et al. [34] introduce a deep learning system for 3D object reconstruction from stereo pairs. However, its dependence on accurate disparity maps limits its performance on real-world data compared to synthetic scenarios. Zhao and Wu [34] utilize 5G to enhance data transmission in a binocular stereo vision system for 3D face modeling. However, its performance is hindered by unknown parallax and varying illumination, requiring further optimization for industrial use. Song et al. [35] propose an online MVS method using MAVs for large-scale 3D reconstruction, improving accuracy through adaptive rescanning and trajectory optimization. However, the method faces challenges such as localization errors, point cloud misalignment, and memory limitations. Yao et al. [36] propose a stereo matching technique that combines sparse high-resolution and dense low-resolution matching for improved efficiency. However, it struggles with occlusions, textureless areas, and artifacts caused by weak sparse matches.

Maryam Sepehrinour and Shohreh Kasaei [24] propose a method for reconstructing the 3D geometry of deformable objects from social network videos, addressing occlusions and lighting variations. However, the method is computationally intensive and lacks evaluation across diverse scenarios. Innmann et al. [25] introduce a non-rigid multi-view stereo (NRMVS) technique for dense 3D reconstruction of dynamic scenes from sparse RGB images. However, it faces challenges with complex scenes, severe deformations, and low-resolution inputs, which affect reconstruction accuracy. Tretschk et al. [37] review advancements in dense monocular non-rigid 3D reconstruction, emphasizing techniques such as neural rendering and 3D Morphable Models. However, they highlight ongoing challenges with clothing deformation tracking and high

computational demands, requiring further research for improved realism and real-time capabilities.

From the above discussion, it is evident that camera path estimation remains a critical challenge in all related research. Accurate path estimation is an essential task for precise 3D reconstruction, as even minor errors in the estimated trajectory can lead to propagated error and may create significant distortions in the final 3D model.

It has been observed that using single camera may not measure the accurate distance of object using SLAM or other model so using of stereo camera may solve this issue in this case . To address this issue, a stereo camera system can be utilized, as it provides precise depth perception by capturing two different perspectives of the scene. This enables accurate distance measurements for each point in the environment. By incorporating a stereo camera model, the proposed approach can effectively correct the camera path by refining both rotation and translation estimations, resulting in a more reliable and accurate 3D model generation.

Another challenge in camera path estimation is the lack of accurate feature extraction and an adequate number of feature points. While Affine SIFT (ASIFT) can be used to address this issue by providing better feature matching under perspective distortions On the otherhand it is computationally expensive. To mitigate this problem, the ASIFT need to be modified according to the requirement by twitching the rotation and tangent parameters according to the requirement. By optimizing the angle estimation for ASIFT, the computational overhead can be significantly reduced, making it more suitable for the requirements of this work while ensuring an increased number of feature matches.

Additionally, the combination of the modified ASIFT and Stereo modeling technique will provide an novel SFM technique to estimate accurate camera movement path estimation. As a result a proper 3D model can be created using the SLAM [1] technique using the generated 3D path.

The rest of the paper is organized as follows: Recent development in this area is depicted in Section 2 by providing the advancement of SFM, SLAM, and Stereo modeling technique. The proposed work is presented in Section 3 and the experimental results are depicted in Section 4. Finally, the paper is concluded in Section 5.

2 Background

Recent developments in computer vision and 3D modeling have completely transformed industries by enabling the visualization of a product and its functionality prior to actual development. This helps in thoroughly analyzing the product even before it is made. Fundamental concepts such as feature estimation, camera movement prediction, 3D modeling, and the stereo camera model are essential to these advancements.

2.1 Feature estimation

2.1.1 SIFT

David Lowe [22] developed the Scale-Invariant Feature Transform (SIFT), a groundbreaking method in computer vision for identifying and describing local features in images [22]. Applications such as motion tracking, object identification, and image stitching all benefit from SIFT. It works by locating distinctive points, or keypoints, that remain unchanged under variations in lighting, scale, or rotation. One fundamental application of SIFT is comparing keypoints across different images. In this process, keypoints are matched based on the similarity of their descriptors. SIFT is capable of handling rotation and scale invariance. However, it struggles with affine transformations. It becomes challenging to identify local maxima and minima in images that have undergone affine transformations.

2.1.2 Affine SIFT

Affine transformations are common in real-world settings, requiring considerable perspective changes, which SIFT finds difficult to handle. In the standard version of ASIFT, the image undergoes some degree of tilt and rotation, which creates an overhead for SIFT extraction and matching.

Morel and Yu [38] created ASIFT, an extension of SIFT, to address these limitations. By simulating various camera orientations, ASIFT enhances SIFT's robustness and enables feature recognition even in the presence of significant perspective fluctuations. ASIFT [38] yields approximately 13.5 times more features for both the query and search images, covering roughly 13.5 times the area of the original images. Consequently, the computational complexity for ASIFT features is roughly 13.5^2 , which equates to approximately 180 times greater than that of SIFT. Despite the higher computational overhead, ASIFT provides an adequate number of consistent match points, which enhances its applicability for dense point cloud generation methods [1].

2.2 Camera movement prediction

A method called SFM [31] can be used to take a series of 2D pictures or video frames and use them to reconstruct the 3D structure of a scene by predicting the relative camera movements. The working method of SFM for two camera positions can be derived using the following steps:

1. First, feature points are estimated from the two views.
2. The matched feature points between the views are identified.
3. Outliers are removed using the RANSAC method.
4. The remaining points are used to compute the Fundamental matrix and the Essential matrix.
5. Using the Essential matrix, the camera rotation and translation coefficients are estimated.

It is clear that the removal of outliers and the identification of inliers are critical steps in the SFM model for calculating the accurate Fundamental and Essential matrices.

2.3 3D modeling

To create an accurate 3D model using SLAM, the camera movement path should be available [1]. In this method, camera triangulation [31] based on re-projection is used to create a point cloud in 3D space. Methods like bundle adjustment [1] are employed to provide an accurate 3D model while utilizing SLAM. The steps involved in bundle adjustment are described below:

1. Collect Input Data: Compile basic camera settings, initial 3D points, and 2D feature points.
2. Initialization: Make preliminary predictions about camera postures and 3D points using SfM or triangulation.
3. Define Cost Function: Calculate the reprojection error between estimated projections and observed 2D points using given equation.

$$\text{Reprojection Error} = \sum_{i=1}^n \sum_{j=1}^m \|x_{ij} - \pi(X_j, P_i)\|^2 \quad (1)$$

where x_{ij} is the observed 2D point of the j -th 3D point in the i -th image, π is the projection function using camera parameters P_i , and X_j is the estimated 3D point.

4. Optimization: Reduce the reprojection error by using the technique like Levenberg-Marquardt [1].
5. Adjust Parameters: Modify 3D points in accordance with optimisation outcomes.
6. Iterate: Continue until the reprojection error has changed very little.
7. Output: Provide precise reconstruction by supplying 3D points.

By reducing reprojection errors and 3D point estimations, bundle adjustment iteratively refines the overall structure to provide a more accurate reconstruction.

2.4 Stereo camera Model

The process of stereo 3D modelling is using stereo pictures taken by two cameras to create a three-dimensional representation of a scene or item. Reconstructing the scene's three-dimensional geometry involves matching corresponding spots in pairs of stereo images. In the process of Stereo camera based 3D modeling, epipole point of the pair of image is taken at $x = \infty$ which makes the movement of all the pixel is in horizontal direction. Now applying the triangulation method with the stereo positioning system, will

provide the accurate distance of each point from the camera with precise horizontal and vertical location. The steps involved in the process of Stereo camera based 3D modeling are described below :

1. Acquire two stereo images of the scene using two calibrated cameras.
2. Preprocessing: it involves two steps
 - Rectify the stereo image pair to align corresponding epipolar lines horizontally.
 - Set the epipole point at $x = \infty$ to ensure horizontal pixel movement.
3. Feature Matching:
 - Detect features in both stereo images using feature detection techniques.
 - Match corresponding points between the two images to establish feature pairs.
4. Validate matched points using the epipolar constraint, ensuring that corresponding points lie on the same epipolar line.
5. Compute the disparity for each pair of matched points:

$$\text{Disparity} = x_{\text{left}} - x_{\text{right}}$$

where x_{left} and x_{right} are the x -coordinates of the matched points in the left and right images, respectively.

6. Use the disparity values, camera baseline (distance between cameras), and focal length to calculate the depth (Z -coordinate) for each point:

$$Z = \frac{f \cdot B}{\text{Disparity}}$$

where f is the focal length, B is the baseline, and Z is the depth.

7. Calculate the horizontal (X) and vertical (Y) coordinates of each point:

$$X = \frac{(x_{\text{left}} - c_x) \cdot Z}{f}$$

$$Y = \frac{(y_{\text{left}} - c_y) \cdot Z}{f}$$

where c_x and c_y are the principal points of the camera.

8. Combine the 3D coordinates (X, Y, Z) for all matched points to reconstruct the 3D model of the scene.
9. Do bundle adjustment to refine the 3D model.

After stereo camera modeling, the distance of each object from Camera 1 (i.e. the left camera) is determined accurately.

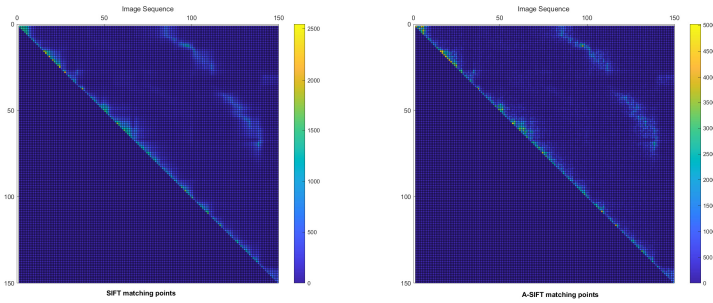


Fig. 1: Comparison of SIFT and ASIFT match points

3 Proposed work

In this proposed work, a stereo camera model is used to create the 3D model. The work is mainly divided into two major parts. In the first part, the camera path is estimated, and in the second part, the estimated camera path is used to create the 3D model. As discussed earlier, accurate camera path estimation is the most challenging task; hence, standard camera path estimation methods may not be applicable.

In this regard, a robust feature estimation model is used in the primary camera path estimation process. The estimated path is then rectified using a stereo modeling technique. As a result, the rectified camera path can be used to create an accurate 3D model in the world coordinate system.

3.1 Camera Path Estimation

As discussed earlier in Section. 2.2, SFM [31] is the most suitable method for estimating the camera path. As explained, finding good inliers is a major concern in estimating accurate camera movement. The acquisition of good inliers is also proportional to a large number of high-quality matching points. In this regard, ASIFT [38] (as discussed in Section. 2.1.2) can be used to fulfill these requirements. In this work, the ASIFT architecture is modified as per the requirements as follows:

- A tilt angle of 15° is applied on the second image to calculate affine feature.
- A rotation angle of 30° is applied second to calculate affine feature.
- SIFT feature points of the first image is matched with the ASIFT feature of the second image

With this modified version of ASIFT, a greater number of good feature points can be estimated compared to traditional SIFT. After that RANSAC model is applied with 10000 trial over the matched feature, to extract the inliers for the camera path estimation. Here, the Figure. 1 shows the comparison of SIFT and ASIFT match points. Intuitively, more inliers can be obtained using more feature matching points. As shown in Figure. 2 it is clear that the number of

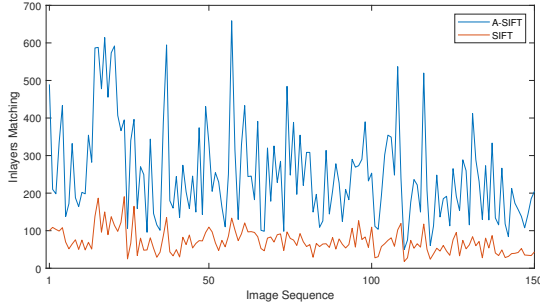


Fig. 2: Comparison of number of Inliers using SIFT and modified ASIFT

inliers is increased after applying the modified ASIFT. After calculating inliers, the fundamental and essential matrix is calculated [31]. Using the essential matrix the relative rotation and relative translation matrix can be calculated. The rotation matrix will provide the rotation angle in X, Y And Z axis as R_x , R_y and R_z subsequently. By multiplying the rotation matrix of the 3 axis, final rotation matrix can be achieved as shown in Eq.2

$$R_{p2c} = R_{(xc)}R_{(yc)}R_{(zc)} \quad (2)$$

where :

C defines the camera C of the stereo camera model and p_1 & p_2 represents the position 1 & position 2. Hence, the n th image at position p_n , the rotation coefficient of the camera can be estimated with respect to the p_{n-1} using the equation stated earlier as Eq.2. To calculate the final rotation coefficient ($R_{(FPnC1)}$) at position p_n with respect to the camera position p_1 , the relative rotation coefficient at p_n (R_{pnc1}) is multiplied with the final rotation coefficient of p_{n-1} . The detail calculation can be carried out using Eq.3.

$$R_{(FPC)} \begin{cases} = R_{(FP-1C)}R_{(PC)} \\ = \begin{bmatrix} 1 & 0 & 0 \\ 0 & 1 & 0 \\ 0 & 0 & 1 \end{bmatrix} \end{cases}, \text{ for } P = 1 \quad (3)$$

where, $R_{(FPC)}$ represents the final rotation of the camera C at position P Similarly, for the camera 2 ($C2$) of the stereo camera model, the final rotation coefficient $R_{(FPnC2)}$ at p_n can be calculated using equation Eq 2 & Eq. 3. Detail steps of the Camera Rotation Estimation is presented in algorithm 5

Algorithm 1 Camera Rotation Estimation**Input:** An Image Sequence at position P=1,2,3,...n. for camera C=1 &2**Output:** Rotation (R) matrix of images P and C**begin**

1. Select Camera C=1
2. Select first image as image 1 (I1) and set rotation as $R_{(FPC)}$ at P=1 as shown in Eq. 3
3. Select next image as image 2 (I2) **for each I2 that is not empty do**
 - (a) Calculate SIFT feature for I1
 - (b) Calculate ASIFT feature for I2.
 - (c) Calculate matching & inliers using RANSAC
 - (d) Calculate Fundamental Matrix using inliers.
 - (e) Calculate Essential Matrix and Rotation coefficient as in Eq. 2
 - (f) Select I1=I2
 - (g) Select I2=next image.
4. Repeat for Camera C=2
5. Return rotation matrix of camera for images as R_{FPC} for P and C= 1 & 2

3.2 Camera Path Correction

After receiving the camera path from SFM model for camera 1 as $R_{(FPC1)}$, rectification is carried out to reduce the negligible errors. As discussed earlier (in Section.2.2) the SFM will generate the relative translation matrix. To ensure accurate camera positioning translation calculation is also an important task. camera path rectification is done using the following methods.

- **Rotation coefficient correction:**

For this SFM has been applied on the stereo camera model and both the rotation coefficient has been averaged to get the final rotation matrix as shown in Eq.4

$$R_{(FP)} = \frac{R_{(FPC1)} + R_{(FPC2)}}{2} \quad (4)$$

where, C1 and C2 represent the camera 1 and camera 2 at position P.

- **Translation coefficient estimation** As shown in Figure. 3 the position 1 for camera 1 and the position 2 for camera 1 is estimated using stereo model technique.

A fixed world point (X,Y,Z) is used for projection, providing a reference point for accurate translation estimation in world coordinate as discussed in Section. 2.4.

Here the world coordinate of the cameras are calculated based on the fixed coordinate point as shown in Figure 3. In different view combination, the fixed world coordinate (object) may not be same. As a result, the camera coordinate win not be consistent. To solve this, the relative camera translation matrix is

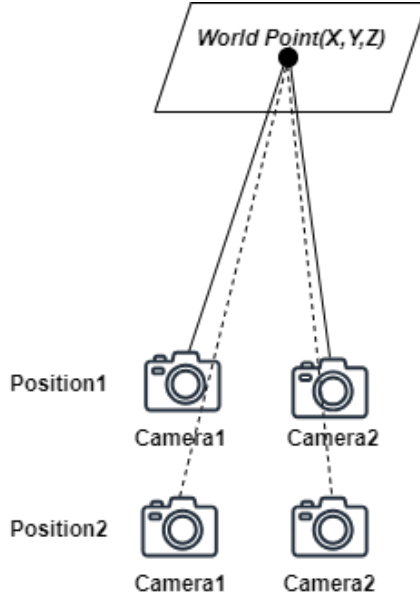


Fig. 3: Stereo camera positioning model

calculated based on each view pairs using the following Eq.5

$$T_P = T_{WP} - T_{WP-1} \quad , for P > 1 \quad (5)$$

where T_{WP} defines the world coordinate position of Camera 1 for world point (X,Y,X) and T_P defines the relative translation as $([T_x \ T_y \ T_z])$. The final camera position is estimated by combining the previous translation coefficient with the current relative translation coefficient as shown in the Eq. 6

$$T_{FP} \left\{ \begin{array}{l} = T_{P-1} + T_P \\ = [0 \ 0 \ 0] \quad , for P = 1 \end{array} \right. \quad (6)$$

where T_{FP} represents the final translation matrix. Detail steps of the Camera Path Correction is presented in algorithm 8.

3.3 Model Creation

After computing the final rotation and translation coefficient (R_{FP} & T_{FP}) for each camera position, model creation is carried out. As discussed in Section. 2.3,

Utilizing triangulation techniques, as commonly employed in SLAM models, we can then generate an accurate 3D model based on the camera's global positioning. This approach allows for precise reconstruction of the scene,

Algorithm 2 Camera Path Correction**Input:** An Image Sequence and R_{FPC} at position

P=1,2,3,...n. for camera C=1 &2.

Output: R_{FP} and T_{FP} where F represents Final Position, P=1,2,3,...n.**begin**

1. Correct the rotation by averaging R_{FPC} for C_1 & C_2 as in equation 4 and calculate R_{FP}
2. Initialise the starting camera position as (0,0,0) for P=1, and select image as I_{1L} and I_{1R} , image left and image right.
3. Calculate the translation of next position using stereo model technique as shown in Figure. 3 using equation 5 as T_P to estimate the final camera position
4. select the next pair of images as I_{2L} and I_{2R} at $P = 2$
5. **for** each P from P=2 to n **do**
 - (a) Calculate the distance of a world fixed point from I_{P-1L} as T_{WP-1}
 - (b) Calculate the distance of a world fixed point from I_{PL} as T_{WP}
6. Calculate the movement as relative translation T_P using equation 5.
7. Add the previous translation to calculate the final translation(T_{FP}) as in equation 6.
8. Return R_{FP} & T_{FP} for each P

ensuring accurate camera localization and 3D mapping. The overall technique has been given in following diagram. Steps for creating create 3D Model is presented in algorithm 3 :

Algorithm 3 3D model creation (I_P, R_{FP}, T_{FP})**Input:** Image sequence, R_{FP}, T_{FP} **Output:** 3D Model**begin**

1. Select the first image to calculate the dense cloud
 - for** $U = 1$ to $(n - 1)$ **do**
 - for** $V = (u + 1) - n$ **do**
 - (a) Calculate dense cloud for I_U & I_v using R_{FP} & T_{FP} ,where P represents U and V
 - (b) Create 3D Model
2. Do bundle adjustment as explained in Section. 2.3

The final workflow of the proposed method is represented in the Figure. 4

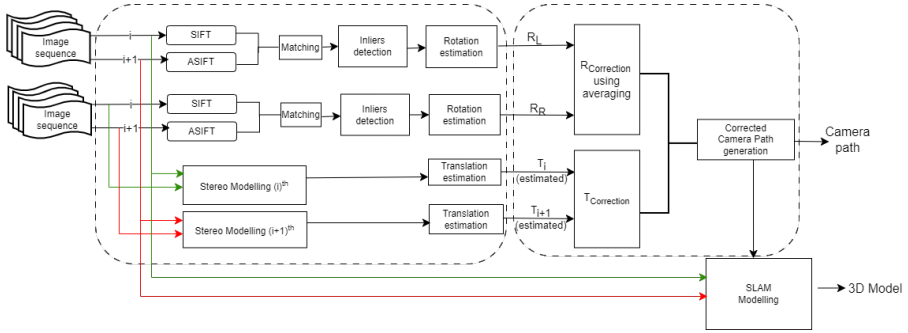


Fig. 4: Proposed model

4 Result and Discussion

4.1 Experimental Setup

In this proposed work, a set of stereo camera is used generate the camera path and 3D model. To validate the resultant path, a proper validation method is required. Hence, experimental setup is divided in dataset generation and validation as follows:

4.1.1 Camera setup

A stereo camera architecture has been used to perform the image capturing for the proposed scheme. The camera setup has been calibrated using the standards 17*9 checkerboard with square of 19.929 mm. Detail camera information for the experiment is represented in Table. 1

Table 1: Experimental Setup

Camera	Resolution	Relative Stereo Parameters
Camera1	1920*1080	$R = \begin{bmatrix} 1 & 0 & 0 \\ 0 & 1 & 0 \\ 0 & 0 & 1 \end{bmatrix}, T = [0 \ 0 \ 0]$
Camera2	1920*1080	$R = \begin{bmatrix} 1 & 0.011 & 0.0163 \\ -0.011 & 1 & 0.008 \\ -0.0162 & -0.008 & 1 \end{bmatrix}$ $T = [-47.917 \ -0.142 \ -13.373]$

4.1.2 Camera Movement Path Validation

To proof the acceptability, ground truth IMU sensor MPU 6050 is used here with 6 axis, 3 axis accelerometer and 3 axis gyroscope which gives proper information on camera trajectory. Here, MPU 6050 is set to collect 100 position points every second [39]. using those points, real camera movement path is generated for validation purpose, allowing for an accurate reconstruction of the real camera movement path.

4.2 Camera path generation and model creations

Using experiment the generated path is calculated and compared with the ground truth (captured using IMU sensor). The detail of camera movement path is shown in Figure. 5

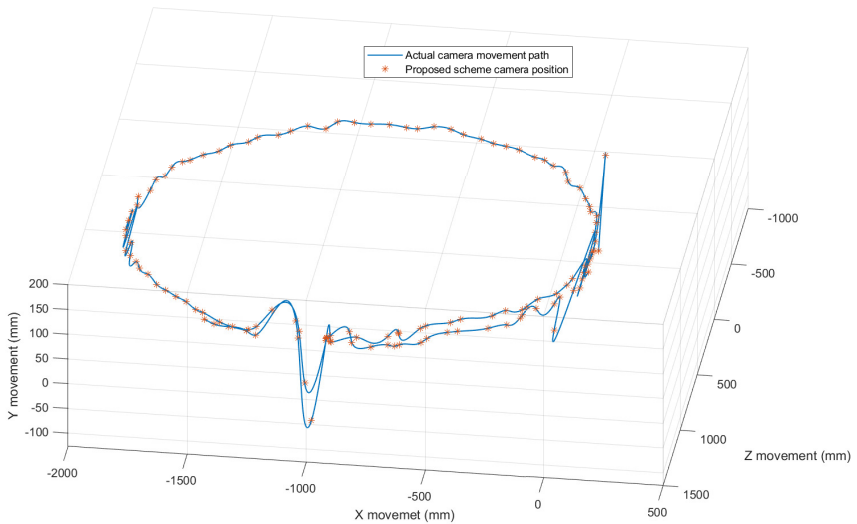


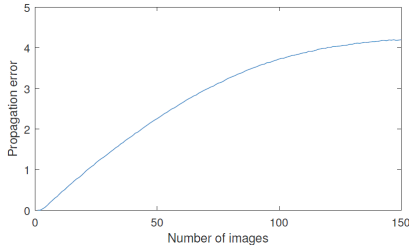
Fig. 5: Actual camera movement path and generated camera movement path using proposed scheme

It is closely observed that after movement of the distance 5120 mm. the proposed scheme gives 4.2 mm error. Also the proposed scheme error is compared with the standard SFM [16], NRSFM [40] as shown in Table 2 The propagated error comparison with existing model is presented in Figure. 6b

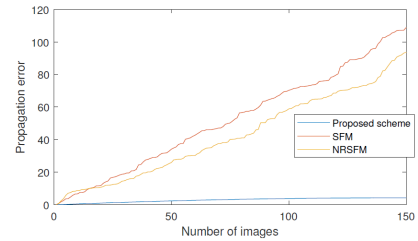
Using the generated camera path using the left and right images [39] (refer to Figure. 7a and Figure. 7b) a 3D model is created as shown in Figure. 7c.

Table 2: Performance comparison with recent approaches

Parameters	Proposed	SFM	NRSFM
Total error (mm)	4.2	108.99	93.69
RMSE (mm)	3.054	60.717	49.589
Accuracy	99.92	97.89	98.19



(a) Proposed model error with movement (in mm)



(b) Comparison of error of proposed model with recent models (in mm)

Fig. 6: Error analysis of the proposed scheme

(a) Sample images (Left) [39]

(b) Sample images (Right) [39]



(c) Generated 3D model

Fig. 7: Generated 3D model using the proposed scheme for the sample left and right images

4.3 Discussion

In this research work, a 3D modeling technique is proposed using a combination of stereo and SFM architecture. It is evident that the proposed path estimation and correction approach significantly improves the camera path generation technique. As a result, the generated model, using the camera

path (via SLAM), provides a precise structure of the target object. In camera path generation, accurately determining the rotation and translation coefficients is the main challenge. Here, using a modified version of ASIFT provides more inlier points for accurately estimating the rotation coefficients. Moreover, stereo-based translation correction provides real-world measurements in relation to the camera position. Each of these techniques was assessed to evaluate its individual and combined effects on performance through a series of carefully monitored tests. The results and benefits of each strategy are discussed below. As discussed in Section 3.1, a rotation angle of 30 degrees and a tilt angle of 15 degrees are applied to enhance affine feature calculation in our model. The computational cost for standard ASIFT is approximately 14 units; however, our approach records a slightly higher computational cost of 16.23 units. This increase is attributed to the integration of standard SIFT alongside ASIFT for feature matching, which contributes to a greater number of matching coefficients. This expanded matching set results in better accuracy than ASIFT. An increased number of matching coefficients, as illustrated earlier in Figure. 1 and Figure. 2, yields a higher number of inliers, leading to a more reliable fundamental matrix F , which subsequently improves the robustness of the model. This larger set of inliers contributes to a more reliable estimation of the rotation matrix R , ensuring better alignment across perspectives. Moreover, our use of a two-camera averaging model for rotation correction, as discussed in Section. 3.2, further enhances accuracy by reducing residual errors introduced by variations in perspective. By averaging rotation data from both cameras, this method minimizes minor errors that might otherwise affect alignment, resulting in a more stable and precise model. In summary, this technique surpasses previous approaches in accuracy and resilience by combining stereo-based rotation and translation correction with ASIFT-based feature matching. The ASIFT algorithm significantly improved the reliability of feature correspondences under challenging viewing conditions, producing approximately 2.5 times more matches than standard SIFT. Furthermore, accurate alignment and error reduction across multiple views were achieved through translation correction anchored by a constant world point and stereo-based rotation correction, accomplished by averaging data from two cameras. Combined, these methods provide a comprehensive and effective solution for high-accuracy 3D model reconstruction, demonstrating clear improvements over traditional techniques, particularly in scenes with complex viewpoints and significant distortions.

5 Conclusion

In this research work, a novel 3D modeling technique has been proposed to create a realistic 3D model with accurate world coordinate measurements using precise camera positioning and a stereo camera modeling technique. The modified version of ASIFT provides more matching points with minimal overhead, enabling the accurate prediction of camera rotation angles along the X, Y, and Z axes. Moreover, the two-camera model-based rotation correction system

ensures precise camera rotation angles. Additionally, the stereo model-based translation prediction and correction technique facilitates smooth camera path generation in 3D world coordinates. As a result, a realistic 3D model can be generated by the SLAM model using the computed camera movement path.

In the future, the 3D models can be used for 3D model-based object detection techniques to overcome the shortcomings of standard object detection. Furthermore, these methods can be applied to 3D inspection purposes.

Declarations

- **Approval of Ethics** There are no trials involving humans or animals in this study.
- **Consent to Participate** Not applicable.
- **Consent to Publish** Not applicable.
- **Data Availability Statement** My manuscript has associated data in a data repository and can be available using the link: <https://data.mendeley.com/preview/jpsch5nftd?a=701be90d-7249-40cd-9eed-a85dab000cd5>
- **Authors Contributions** Both the authors contributed equally to this work.
- **Funding** The authors declare that no funding was received for conducting this research.
- **Competing interests** There are no conflicts of interest related to this research, according to the authors.

References

- [1] Taheri, H., Xia, Z.C.: Slam; definition and evolution. *Engineering Applications of Artificial Intelligence* **97**, 104032 (2021)
- [2] Zheng, J.Y., Fukagawa, Y., Abe, N.: 3d surface estimation and model construction from specular motion in image sequences. *IEEE Transactions on Pattern Analysis and Machine Intelligence* **19**(5), 513–520 (1997)
- [3] Bodor, R., Schrater, P., Papanikolopoulos, N.: Multi-camera positioning to optimize task observability. In: *IEEE Conference on Advanced Video and Signal Based Surveillance, 2005.*, pp. 552–557 (2005). IEEE
- [4] Lu, F., Milios, E.: Globally consistent range scan alignment for environment mapping. *Autonomous robots* **4**, 333–349 (1997)
- [5] Thrun, S., Montemerlo, M.: The graph slam algorithm with applications to large-scale mapping of urban structures. *The International Journal of Robotics Research* **25**(5-6), 403–429 (2006)
- [6] Davison, A.J., Reid, I.D., Molton, N.D., Stasse, O.: Monoslam: Real-time single camera slam. *IEEE transactions on pattern analysis and machine*

- intelligence **29**(6), 1052–1067 (2007)
- [7] Brian, W.: Real-time slam relocalisation. Proc. of ICCV2007 (2007)
- [8] Strasdat, H., Montiel, J.M., Davison, A.J.: Visual slam: why filter? Image and Vision Computing **30**(2), 65–77 (2012)
- [9] Mur-Artal, R., Montiel, J.M.M., Tardos, J.D.: Orb-slam: a versatile and accurate monocular slam system. IEEE transactions on robotics **31**(5), 1147–1163 (2015)
- [10] Sandström, E., Li, Y., Van Gool, L., Oswald, M.R.: Point-slam: Dense neural point cloud-based slam. In: Proceedings of the IEEE/CVF International Conference on Computer Vision, pp. 18433–18444 (2023)
- [11] Torresani, L., Hertzmann, A., Bregler, C.: Learning non-rigid 3d shape from 2d motion. Advances in neural information processing systems **16** (2003)
- [12] Fayad, J., Del Bue, A., Agapito, L., Aguiar, P.: Non-rigid structure from motion using quadratic deformation models. In: BMVC, vol. 1, p. 2 (2009). Citeseer
- [13] Gotardo, P.F., Martinez, A.M.: Non-rigid structure from motion with complementary rank-3 spaces. In: CVPR 2011, pp. 3065–3072 (2011). IEEE
- [14] Kumar, S., Dai, Y., Li, H.: Multi-body non-rigid structure-from-motion. In: 2016 Fourth International Conference on 3D Vision (3DV), pp. 148–156 (2016). IEEE
- [15] Sengupta, A., Bartoli, A.: Colonoscopic 3d reconstruction by tubular non-rigid structure-from-motion. International Journal of Computer Assisted Radiology and Surgery **16**(7), 1237–1241 (2021)
- [16] Westoby, M.J., Brasington, J., Glasser, N.F., Hambrey, M.J., Reynolds, J.M.: ‘structure-from-motion’ photogrammetry: A low-cost, effective tool for geoscience applications. Geomorphology **179**, 300–314 (2012)
- [17] Martínez-Espejo Zaragoza, I., Caroti, G., Piemonte, A., Riedel, B., Tengen, D., Niemeier, W.: Structure from motion (sfm) processing of uav images and combination with terrestrial laser scanning, applied for a 3d-documentation in a hazardous situation. Geomatics, Natural Hazards and Risk **8**(2), 1492–1504 (2017)
- [18] Yuan, Y., Ding, Y., Zhao, L., Lv, L.: An improved method of 3d scene reconstruction based on sfm. In: 2018 3rd International Conference on

- Robotics and Automation Engineering (ICRAE), pp. 228–232 (2018). IEEE
- [19] Nesbit, P., Hugenholtz, C.: Enhancing UAV–SfM 3D model accuracy in high-relief landscapes by incorporating oblique images. *Remote Sens* 11: 239 (2019)
- [20] Xiao, Y., Xue, N., Wu, T., Xia, G.-S.: Level-sfm: Structure from motion on neural level set of implicit surfaces. In: *Proceedings of the IEEE/CVF Conference on Computer Vision and Pattern Recognition*, pp. 17205–17214 (2023)
- [21] Chen, Q., Poullis, C.: End-to-end multi-view structure-from-motion with hypercorrelation volume. In: *2023 IEEE 3rd International Conference on Power, Electronics and Computer Applications (ICPECA)*, pp. 1300–1303 (2023). IEEE
- [22] Lowe, D.G.: Object recognition from local scale-invariant features. In: *Proceedings of the Seventh IEEE International Conference on Computer Vision*, vol. 2, pp. 1150–1157 (1999). Ieee
- [23] Du, H., Yan, X., Wang, J., Xie, D., Pu, S.: Rethinking the approximation error in 3d surface fitting for point cloud normal estimation. In: *Proceedings of the IEEE/CVF Conference on Computer Vision and Pattern Recognition*, pp. 9486–9495 (2023)
- [24] Sepehrinour, M., Kasaei, S.: 3d reconstruction of non-rigid surfaces from realistic monocular video. In: *2015 9th Iranian Conference on Machine Vision and Image Processing (MVIP)*, pp. 199–202 (2015). IEEE
- [25] Innmann, M., Kim, K., Gu, J., Nießner, M., Loop, C., Stamminger, M., Kautz, J.: Nrmvs: Non-rigid multi-view stereo. In: *Proceedings of the IEEE/CVF Winter Conference on Applications of Computer Vision*, pp. 2754–2763 (2020)
- [26] Aziz, S., Ahmed, M., Naqvi, S.Z.H., Khan, M.U., Imtiaz, A., Waseem, A.: Machine bearing fault diagnosis system using tri-axial accelerometer. In: *2020 International Conference on Electrical, Communication, and Computer Engineering (ICECCE)*, pp. 1–6 (2020). IEEE
- [27] Ware, C., Osborne, S.: Exploration and virtual camera control in virtual three dimensional environments. In: *Proceedings of the 1990 Symposium on Interactive 3D Graphics*, pp. 175–183 (1990)
- [28] Hachet, M., Declé, F., Knodel, S., Guitton, P.: Navidget for easy 3d camera positioning from 2d inputs. In: *2008 IEEE Symposium on 3D User Interfaces*, pp. 83–89 (2008). Ieee

- [29] Arif, O., Vela, P.A.: Non-rigid object localization and segmentation using eigenspace representation. In: 2009 IEEE 12th International Conference on Computer Vision, pp. 803–808 (2009). IEEE
- [30] Jaffré, G., Crouzil, A.: Non-rigid object localization from color model using mean shift. In: Proceedings 2003 International Conference on Image Processing (Cat. No. 03CH37429), vol. 3, p. 317 (2003). IEEE
- [31] Granshaw, S.I.: Structure from motion: origins and originality. Wiley Online Library (2018)
- [32] Tulsiani, S., Tucker, R., Snavely, N.: Layer-structured 3d scene inference via view synthesis. In: Proceedings of the European Conference on Computer Vision (ECCV), pp. 302–317 (2018)
- [33] Wang, Y., Yang, B., Hu, R., Liang, M., Urtasun, R.: Plumenet: Efficient 3d object detection from stereo images. In: 2021 IEEE/RSJ International Conference on Intelligent Robots and Systems (IROS), pp. 3383–3390 (2021). IEEE
- [34] Xie, H., Yao, H., Zhou, S., Zhang, S., Tong, X., Sun, W.: Toward 3d object reconstruction from stereo images. *Neurocomputing* **463**, 444–453 (2021)
- [35] Song, S., Kim, D., Choi, S.: View path planning via online multiview stereo for 3-d modeling of large-scale structures. *IEEE Transactions on Robotics* **38**(1), 372–390 (2021)
- [36] Yao, C., Jia, Y., Di, H., Li, P., Wu, Y.: A decomposition model for stereo matching. In: Proceedings of the IEEE/CVF Conference on Computer Vision and Pattern Recognition, pp. 6091–6100 (2021)
- [37] Tretschk, E., Kairanda, N., BR, M., Dabral, R., Kortylewski, A., Egger, B., Habermann, M., Fua, P., Theobalt, C., Golyanik, V.: State of the art in dense monocular non-rigid 3d reconstruction. In: Computer Graphics Forum, vol. 42, pp. 485–520 (2023). Wiley Online Library
- [38] Yu, G., Morel, J.-M.: ASIFT: An Algorithm for Fully Affine Invariant Comparison. *Image Processing On Line* **1**, 11–38 (2011). <https://doi.org/10.5201/ipol.2011.my-asift>
- [39] RANA, S., Kumari, U.: Stereo-SFM Modelling Dataset. Mendeley (2025). <https://doi.org/10.17632/jpsch5nftd.1>. <https://data.mendeley.com/preview/jpsch5nftd?a=701be90d-7249-40cd-9eed-a85dab000cd5>
- [40] Kumar, S., Van Gool, L., de Oliveira, C.E., Cherian, A., Dai, Y., Li, H.: Dense non-rigid structure from motion: A manifold viewpoint. arXiv preprint arXiv:2006.09197 (2020)